

Radiation damage effect on photodesorption rates from astronomical ices

Chunqing Yuan¹

University of Virginia

Department of Chemistry, McCormick Rd, Charlottesville, VA 22903, USA

E-mail: cy3cy@virginia.edu

John T. Yates, Jr.

University of Virginia

Department of Chemistry, McCormick Rd, Charlottesville, VA 22903, USA

E-mail: jty2n@virginia.edu

Photodesorption from an interstellar CO₂ (ice) analogue at 75K has been studied using Lyman- α (10.2 eV) radiation. We combine quantitative mass spectrometric studies of gases evolved and transmission IR studies of species trapped in the ice. Direct CO desorption is observed from the primary CO₂ photodissociation process which occurs promptly for CO₂ molecules located on the outermost surface of the ice (Process I). As the fluence of Lyman- α radiation increases to $\sim 5.5 \times 10^{17}$ photons cm⁻², extensive damage to the crystalline ice occurs, and photo-produced CO molecules from deeper regions (Process II) are found to desorb at a rapidly-increasing rate which becomes two orders of magnitude greater than Process I. It is postulated that deep radiation damage to produce an extensive amorphous phase of CO₂ occurs in the 50 nm ice film and that CO (and CO₂) diffusive transport is strongly enhanced in the amorphous phase. Photodesorption in Process II is a combination of electronic and thermally activated processes. Radiation damage in crystalline CO₂ ice has been monitored by its effects on the vibrational lineshapes of CO₂(ice). Here the crystalline-to-amorphous phase transition has been correlated with the occurrence of efficient molecular transport over long distance through the amorphous phase of CO₂ (ice). Future studies of the composition of interstellar molecular clouds generated by photodesorption from ice layers on dust grains will have to consider the significant effects of radiation damage on photodesorption rates.

*The Life Cycle of Dust in the Universe: Observations, Theory, and Laboratory Experiments (LCDU 2013)
November 18-22, 2013
Taipei, Taiwan*

¹Speaker

1. Introduction

Photodesorption from ices is thought to be a source of gas phase molecules in the interstellar medium (ISM)[1-4]. The destructive interaction between extreme ultraviolet (EUV) radiation and ices has been shown to greatly enhance the rate of photodesorption; it is believed that irradiation with photons or electrons will cause photosensitive ices to become more porous and to exhibit weaker intermolecular bonding as crystal disorder is produced[5]. It has been observed in several studies of photodesorption from ices that an induction period occurs at the beginning of irradiation[6, 7]. This delayed onset of the rapid evolution of photoproducts is thought to be due to photon-induced ice disordering related to the photodecomposition and desorption of a fraction of the molecules composing the ice. Radiation induced changes in the ice structure influences the photodesorption rate of molecules as well as the trapping of photoproducts.

In this report we show that large structural changes in the CO₂ (ice) occur during Lyman- α induced photochemistry. In a CO₂ ice film at 75 K, radiation damage increases the CO photodesorption rate by ~ 90 fold and the CO₂ photodesorption rate by ~ 8 fold. These effects are only observed readily using a type of photodesorption measurement particularly sensitive to the kinetics of desorption from the ice surface. We demonstrate that radiation damage, causing crystal structure disorder to ices, produces new more efficient molecular transport pathways which are accessed by photoexcitation processes. Such radiation damage effects will therefore have to be considered in models concerned with the gas phase composition of regions of the ISM where photodesorption from ices is a major factor in supplying gas phase products.

2. Experimental

The experiment was carried out in a stainless steel high-vacuum cell with a base pressure of 1×10^{-8} Torr, as described in detail previously [8-10]. Transmission IR spectroscopy is employed to measure the change of the CO₂ (ice) absorption spectra and the formation of new species during irradiation. The Lyman- α irradiation (10.2 eV; $(2.7 \pm 0.7) \times 10^{14}$ photons \cdot cm⁻² \cdot s⁻¹) is produced by an rf-activated hydrogen discharge lamp and transmitted through a MgF₂ window [8, 11]. In a typical measurement, a nominal 50 nm CO₂ ice film is condensed at 75 K as a crystalline ice [12] onto a KBr plate produced by compression of KBr powder into a W grid. This method of support for the ice gives very efficient thermal contact between the grid, the KBr support and the ice film as well as excellent IR transmission. The characteristic (1/e) penetration depth of Lyman- α photons in CO₂ (ice) is measured to be approximately 50 nm [9]; therefore about 2/3 of the incident light irradiation is absorbed by the ice film. The cell is always open to a turbo molecular pump and an ion pump with a combined constant pumping speed, S (for CO, S_{CO}=0.21 L \cdot s⁻¹; for CO₂, S_{CO₂}=0.19 L \cdot s⁻¹). This accurate direct measurement of pumping speed in the cell allows us to use partial pressure measurements during irradiation to quantitatively measure the photodesorption rates as a function of exposure of the ice film to radiation.

3. Results

The photodissociation of $^{13}\text{CO}_2$ ice produces ^{13}CO , $^{13}\text{CO}_3$ and other trapped products, as described elsewhere[9]. Figure 1(a) shows the rate of production of $^{13}\text{CO}(\text{g})$ vs. time, using the QMS. When the shutter is opened, the partial pressure of $^{13}\text{CO}(\text{g})$ immediately jumped up by a small amount. This is called Process I. Process I is accompanied by a slow growth in $^{13}\text{CO}(\text{g})$ pressure in the induction period and more rapid growth beyond called Process II. An increasingly rapid rate of evolution of $^{13}\text{CO}(\text{g})$ is detected as Process II develops beyond the induction period. However, as shown in Figure 1(b) and (c), the production of trapped ^{13}CO and $^{13}\text{CO}_3$ molecules in the matrix as measured by IR occurs by entirely different kinetics: $^{13}\text{CO}(\text{Tr})$ and $^{13}\text{CO}_3(\text{Tr})$ begin to form promptly in a process which is initially linear with radiation time, and with no observable induction period. Figure 1(d) shows the photodepletion of $^{13}\text{CO}_2$ (ice) as measured by IR spectroscopy. The $^{13}\text{CO}_2$ photodepletion rate is almost linear with respect to radiation time over the whole range and no significant induction period is observed.

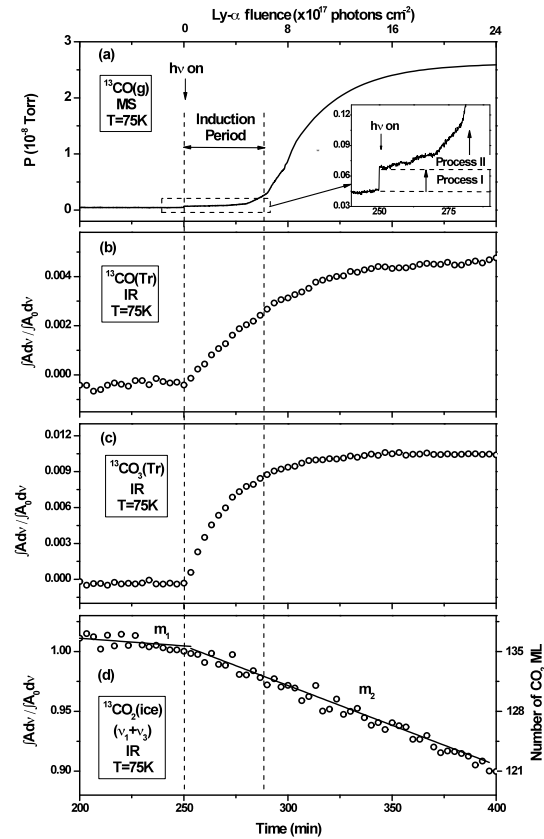


Figure 1: IR and QMS measurement of CO_2 ice and irradiation products.

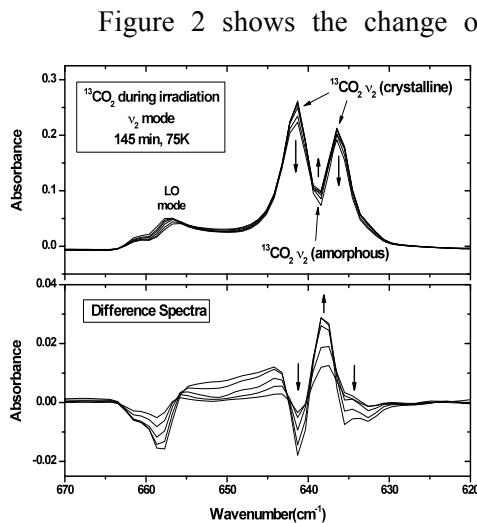


Figure 2: The ν_2 mode of $^{13}\text{CO}_2$ (ice) during irradiation at 75K.

Figure 2 shows the change of the ν_2 bending mode spectrum of CO_2 (ice) during irradiation. The ν_2 mode is also a characteristic mode for distinguishing crystalline and amorphous CO_2 (ice). In crystalline $^{13}\text{CO}_2$ (ice) there are two sharp bands at 641 and 636 cm^{-1} , while amorphous ice exhibits only one broad band at around 640 cm^{-1} [12]. During irradiation, the crystalline double bands decrease during irradiation, and a new band related to the formation of amorphous $\text{CO}_2(\text{ice})$ increases in between them. This observation shows that Lyman- α irradiation changes crystalline $\text{CO}_2(\text{ice})$ into an amorphous phase. Similar radiation-induced phase transitions have also been observed in water ices [5].

Figure 3 shows a schematic diagram of a sandwich structure of $^{12}\text{CO}_2$ (ice) on top of $^{13}\text{CO}_2$ (ice) made by sequential deposition of 25 nm of each isotopomer at 75 K. Two observations in Figure 3 may be made for the sandwich structure: (1). Process I is essentially absent from the sandwich ice structure for ^{13}CO evolution as a result of the presence of a 25 nm $^{12}\text{CO}_2$ capping layer; (2). Process II efficiently delivers ^{13}CO from the under layer to the gas phase for the radiation-damaged $\text{CO}_2(\text{ice})$. The second observation strongly indicates that deep radiation damage is occurring during Process II and that this damage extends over the 50 nm depth of the film, even in the early stages of Process II.

4. Discussion

Process I, shown in Figure 1(a), is a prompt process which develops to completion immediately when the $\text{CO}_2(\text{ice})$ surface first receives Lyman- α photons. This process is caused by the photodecomposition of CO_2 molecules accompanied by fast loss of CO to the gas phase. The promptness of Process I and its small magnitude suggests that it does not involve thermally-activated CO transport steps but is a direct photoprocess originating from the outermost surface-bound CO_2 molecules. As shown in Figure 3, Process I can be significantly attenuated by the adsorption of another crystalline isotopic $\text{CO}_2(\text{ice})$ layer on the surface.

The enormous enhancement of the CO (and CO_2) desorption rate during Process II is related to radiation-induced lattice damage to the CO_2 lattice. The dissociation fragment species carry several eV of kinetic energy and cause long range damage to crystalline $\text{CO}_2(\text{ice})$. The conversion of crystalline $\text{CO}_2(\text{ice})$ to amorphous ice is postulated on the basis of the vibrational spectral changes observed as radiation damage builds up. In the induction period each $\text{CO}_2(\text{ice})$ molecule has absorbed on average 4 Lyman- α photons. This leads one to conclude that massive ice damage is occurring in this experiment. The production of an amorphous CO_2 phase by radiation damage in $\text{CO}_2(\text{ice})$ favors CO and CO_2 transport through the ice and then to vacuum.

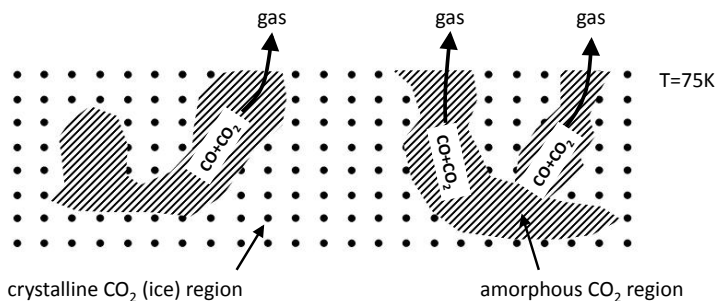


Figure 4: Schematic cross section of crystalline CO_2 (ice) containing large interconnected radiation-induced amorphous regions which strongly favor CO mobility and desorption over a wide spatial range.

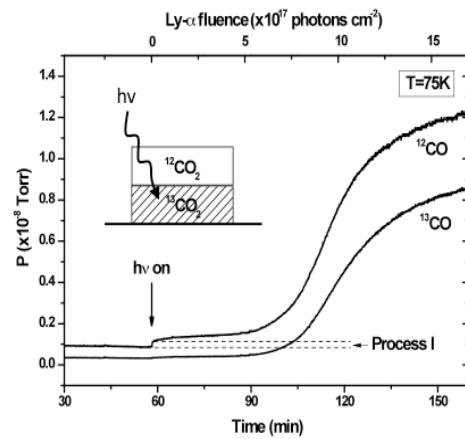


Figure 3: Comparison of ^{12}CO and ^{13}CO evolution from a 25 nm film of $^{12}\text{CO}_2(\text{ice})$ on top of a 25 nm film of $^{13}\text{CO}_2(\text{ice})$ during irradiation.

A similar effect of enhanced diffusion in amorphous solid water vs. crystalline ice has been observed, where amorphous-water ice exhibits $\sim 10^6$ greater H_2O diffusivity than crystalline ice near 155K[13].

The desorption of CO and CO_2 from the ice is strongly enhanced by the ice conversion from crystalline ice to amorphous

ice by radiation damage. Figure 4 shows a schematic diagram of CO₂ (ice) in which interconnected amorphous regions are produced by radiation damage, forming spatially extensive and efficient channels for rapid CO transport throughout the ice thickness. As these channels penetrate the CO₂ (ice) and reach the ice surface, rapid desorption of CO occurs from the channel ends and the CO desorption rate is enhanced by orders of magnitude as a result of exit channel formation, delivering mobile CO molecules from sites in the bulk to the surface.

5. Summary

For CO₂(ice) at 75 K, an induction period for the development of the full CO photo-desorption rate is observed. Here mainly CO₂ (ice) photodissociation from surface CO₂ molecules occurs, yielding CO and O by a prompt process (Process I). As radiation damage in the CO₂ (ice) develops, a rapid CO photodesorption process (Process II) is observed to develop and to increase the rate of CO desorption by about 90-fold over Process I. The great enhancement of the CO and CO₂ desorption rate from the CO₂ (ice) surface in Process II is shown to be due to radiation damage deep in the CO₂(ice). Amorphous CO₂(ice) production, leading to an interconnected amorphous phase, provides extremely facile pathways for mobile CO and CO₂ molecules to exit from the surface, compared to transport through crystalline ice.

References

- [1] Willacy, K. and W.D. Langer, *Astrophys. J.*, 2000. **544**: p. 903.
- [2] Öberg, K.I., et al., *Astrophys. J.*, 2007. **662**: p. L23.
- [3] Hogerheijde, M.R., et al., *Science*, 2011. **334**: p. 338.
- [4] Caselli, P., et al., *Astrophys. J.*, 2012. **759**: p. L37.
- [5] Leto, G. and G.A. Baratta, *Astron. Astrophys.*, 2003. **397**: p. 7.
- [6] Öberg, K.I., E.F. van Dishoeck, and H. Linnartz, *Astron. Astrophys.*, 2009. **496**: p. 281.
- [7] Bahr, D.A. and R.A. Baragiola, *Astrophys. J.*, 2012. **761**: p. 36.
- [8] Rajappan, M., C. Yuan, and J.T. Yates, Jr., *J. Chem. Phys.*, 2011. **134**: p. 064315.
- [9] Yuan, C. and J.T. Yates, Jr., *J. Chem. Phys.*, 2013. **138**: p. 154302.
- [10] Yuan, C. and J.T. Yates, Jr., *J. Chem. Phys.*, 2013. **138**: p. 154303.
- [11] Rajappan, M., et al., *J. Phys. Chem. A*, 2010. **114**: p. 3443.
- [12] Falk, M., *J. Chem. Phys.*, 1987. **86**: p. 560.
- [13] Smith, R.S., C. Huang, and B.D. Kay, *J. Phys. Chem. B*, 1997. **101**: p. 6123.